Cell

Activity-Dependent IGF-1 Exocytosis Is Controlled by the Ca^{2+}-Sensor Synaptotagmin-10

Peng Cao,[1] Anton Maximov,[2,3] and Thomas C. Südhof[1,2,*]
[1]Department of Molecular and Cellular Physiology, and Howard Hughes Medical Institute, Stanford University, 1050 Arastradero Rd., Palo Alto, California 94305, USA
[2]Department of Neuroscience and Molecular Genetics, and Howard Hughes Medical Institute, UT Southwestern Medical Center, Dallas, TX 75390, USA
[3]Present address: Dorris Neuroscience Center, Department of Cell Biology, The Scripps Research Institute, La Jolla, CA 92037, USA
*Correspondence: tcs1@stanford.edu
DOI 10.1016/j.cell.2011.03.034

SUMMARY

Synaptotagmins Syt1, Syt2, Syt7, and Syt9 act as Ca^{2+}-sensors for synaptic and neuroendocrine exocytosis, but the function of other synaptotagmins remains unknown. Here, we show that olfactory bulb neurons secrete IGF-1 by an activity-dependent pathway of exocytosis, and that Syt10 functions as the Ca^{2+}-sensor that triggers IGF-1 exocytosis in these neurons. Deletion of Syt10 impaired activity-dependent IGF-1 secretion in olfactory bulb neurons, resulting in smaller neurons and an overall decrease in synapse numbers. Exogenous IGF-1 completely reversed the Syt10 knockout phenotype. Syt10 colocalized with IGF-1 in somatodendritic vesicles of olfactory bulb neurons, and Ca^{2+}-binding to Syt10 caused these vesicles to undergo exocytosis, thereby secreting IGF-1. Thus, Syt10 controls a previously unrecognized pathway of Ca^{2+}-dependent exocytosis that is spatially and temporally distinct from Ca^{2+}-dependent synaptic vesicle exocytosis controlled by Syt1. Our findings thereby reveal that two different synaptotagmins can regulate functionally distinct Ca^{2+}-dependent membrane fusion reactions in the same neuron.

INTRODUCTION

Studies spanning two decades have identified synaptotagmin-1 (Syt1) and three of its close homologs, Syt2, Syt7, and Syt9, as Ca^{2+}-sensors for fast synaptic and neuroendocrine exocytosis (reviewed in Gustavsson and Han, 2009). Synaptotagmins are vesicle proteins composed of a short N-terminal intravesicular sequence followed by a single transmembrane region, a linker sequence, and two C-terminal C_2-domains that bind Ca^{2+} in some but not all synaptotagmins. Ca^{2+} induces binding of the two Syt1 C_2-domains to phospholipid membranes and to assembled SNARE-complexes; both actions contribute to triggering exocytosis (Fernandez-Chacon et al., 2001; Pang et al., 2006).

However, in addition to the well-characterized exocytotic Ca^{2+}-sensors Syt1, Syt2, Syt7 and Syt9, mammals express four other Ca^{2+}-binding synaptotagmins whose function remains unknown (Syt3, Syt5, Syt6, and Syt10). Strikingly, Syt3, Syt5, Syt6, and Syt10 constitute a separate class of synaptotagmins with homologous N-terminal cysteine residues that form disulfide bonds, thereby dimerizing these synaptotagmins (Fukuda et al., 1999). Syt3, Syt5, Syt6, and Syt10 exhibit similar Ca^{2+}-dependent phospholipid- and SNARE-binding properties as Syt1, although with a higher apparent Ca^{2+}-affinity (Li et al., 1995a and 1995b; Sugita et al., 2002), form a tight complex with assembled SNARE complexes in a manner reminiscent of Syt1 (Vrljic et al., 2010), and promote Ca^{2+}-dependent liposome fusion in vitro (Bhalla et al., 2008). The properties of Syt3, Syt5, Syt6, and/or Syt10 suggest that they act as Ca^{2+}-sensors for some form of exocytosis, possibly asynchronous neurotransmitter release (Li et al., 1995b), but no loss-of-function experiments to probe their biological roles have been reported.

In brain, Syt3, Syt5, Syt6, and Syt10 are primarily, maybe exclusively, expressed in neurons (Mittelstaedt et al., 2009). Syt3 and Syt5 are widely distributed, whereas Syt6 is primarily expressed in layer 5 pyramidal neurons of the cortex, and Syt10 in olfactory bulb neurons (Mittelstaedt et al., 2009). Interestingly, expression of Syt10 but not of Syt3, Sy5, or Syt6 is induced in cortex by seizures (Babity et al., 1997). In the present study, we have systematically examined the function of Syt10, chosen because of its localization to the olfactory bulb, using a genetic approach. Surprisingly, our data show that Syt10 functions as a Ca^{2+}-sensor for the exocytotic secretion of IGF-1 containing vesicles, and that this role is specific for Syt10, whereas Syt1 acts as a separate Ca^{2+}-sensor for exocytosis of synaptic vesicles in the same neurons. Our data define an unanticipated Ca^{2+}-dependent secretory pathway in neurons that coexists with the standard synaptotagmin-dependent synaptic and neuroendocrine pathways of exocytosis; thus, different synaptotagmins can in the same cell control distinct Ca^{2+}-triggered

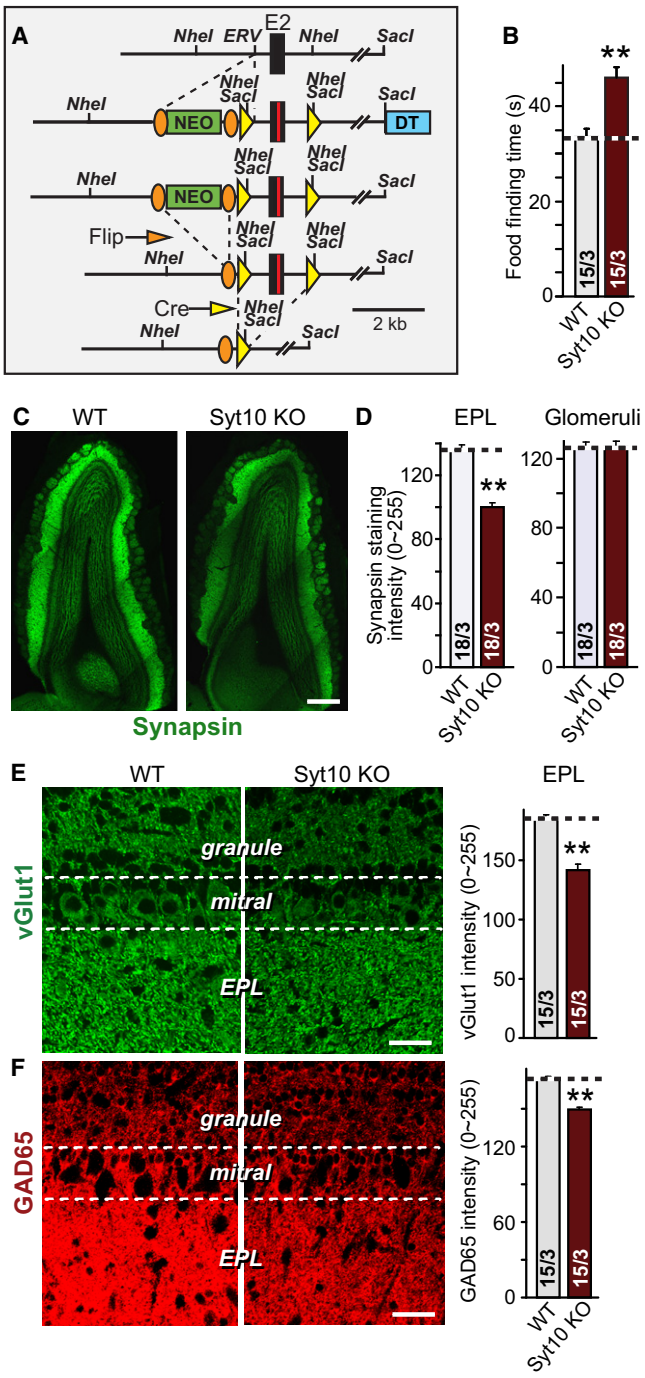

Figure 1. Syt10 KO Impairs Food-Finding Behavior and Decreases Olfactory Bulb Synapse Numbers

(A) Schematic diagram of the generation of conditional and constitutive Syt10 KO mice. Positions of selected restriction enzymes and of coding exon 2 (E2) as well as of frt (orange ovals) and loxP recombination sites (yellow triangles) are indicated (NEO, neomycin resistance cassette; DT, diphtheria toxin). Note that the mutagenesis scheme generates both conditional and constitutive Syt10 KO mice. (B) Constitutive Syt10 KO mice exhibit impaired food-finding behaviors. Summary graph shows mean time (±SEM) required for littermate wild-type and Syt10 KO mice to find a buried cookie. For survival and weight measurements, see Figures S1A and S1B.

(C and D) Representative image (C) and summary graphs of the overall staining intensity (D) of olfactory bulbs from littermate wild-type and constitutive Syt10 KO mice labeled by indirect immunofluorescence for the presynaptic protein synapsin. Note the decrease in synapsin staining in the external plexiform layer (EPL) but not the glomerular layer of Syt10 KO mice (scale bar = 0.4 mm).

(E and F) Representative images (left panels) and summary graphs of the staining intensity in the EPL (right panels) of olfactory bulbs from littermate wild-type and Syt10 KO mice analyzed by labeling for the excitatory presynaptic protein vGlut1 (E) and the inhibitory presynaptic protein GAD65 (F). The EPL was analyzed because it is the major synaptic layer in olfactory bulb that contains the reciprocal mitral/granule cell synapses. Note that measurements of neuronal densities and synapse densities in the glomerular layer found no change (Figures S1E–S1I). Scale bars represent 50 μm.

All summary graphs show means ± SEMs; number of sections/number of mice are shown in individual bars. Statistical analyses were performed by Student's t test comparing KO with wild-type samples (**$p < 0.01$). See also Table S1.

exocytosis reactions that operate without overlap, but by similar mechanisms.

RESULTS

Syt10 KO Impairs Food-Finding Behaviors and Decreases Olfactory Bulb Synapse Numbers

We produced constitutive and conditional Syt10 KO mice by homologous recombination in embryonic stem cells (Figure 1A). Constitutive Syt10 KO mice were viable and fertile (Figures S1A and S1B). Since Syt10 is expressed at highest levels in the olfactory bulb (Mittelstaedt et al., 2009), we examined whether deletion of Syt-10 impairs olfaction. When compared to wild-type littermate controls, Syt10 KO mice exhibited a significant increase in the time required to find hidden food, suggesting that their olfactory function is decreased (Figure 1B).

We next studied the olfactory bulb of Syt10 KO mice anatomically. We found no change in overall gross morphology (Figure 1C) and no alteration in the density of mitral and granule cell neurons (Figures S1C and S1D). However, measurements of the staining intensity for synapsin, a general synaptic marker (Südhof et al., 1989), revealed that the synapsin signal was decreased in the external plexiform layer (EPL), but not the olfactory glomeruli (Figures 1C and 1D and Figure S1E). To investigate this further, we measured the overall density of excitatory and inhibitory synapses in the EPL using antibodies to the vesicular glutamate transporter (vGlut1) and to glutamic acid decarboxylase-65 (GAD65), respectively (Figures 1E and 1F and Figures S1F–S1I). Both markers revealed a significant reduction of staining intensity over the EPL but not the olfactory glomeruli, suggesting that the Syt10 KO decreases the overall density of synapses in the EPL.

Syt10 KO Impairs Synaptic Transmission in the Olfactory Bulb as Measured by Acute Slice Physiology

Most synapses in the EPL are reciprocal dendrodendritic synapses between excitatory mitral cell neurons and inhibitory granule cell neurons (Isaacson and Strowbridge, 1998; Schoppa et al., 1998; Chen and Shepherd, 1997). Their overall function can be monitored in acute olfactory bulb slices by stimulating extracellularly in the granule cell layer, and recording in whole-cell mode from mitral neurons (Chen and Shepherd, 1997;

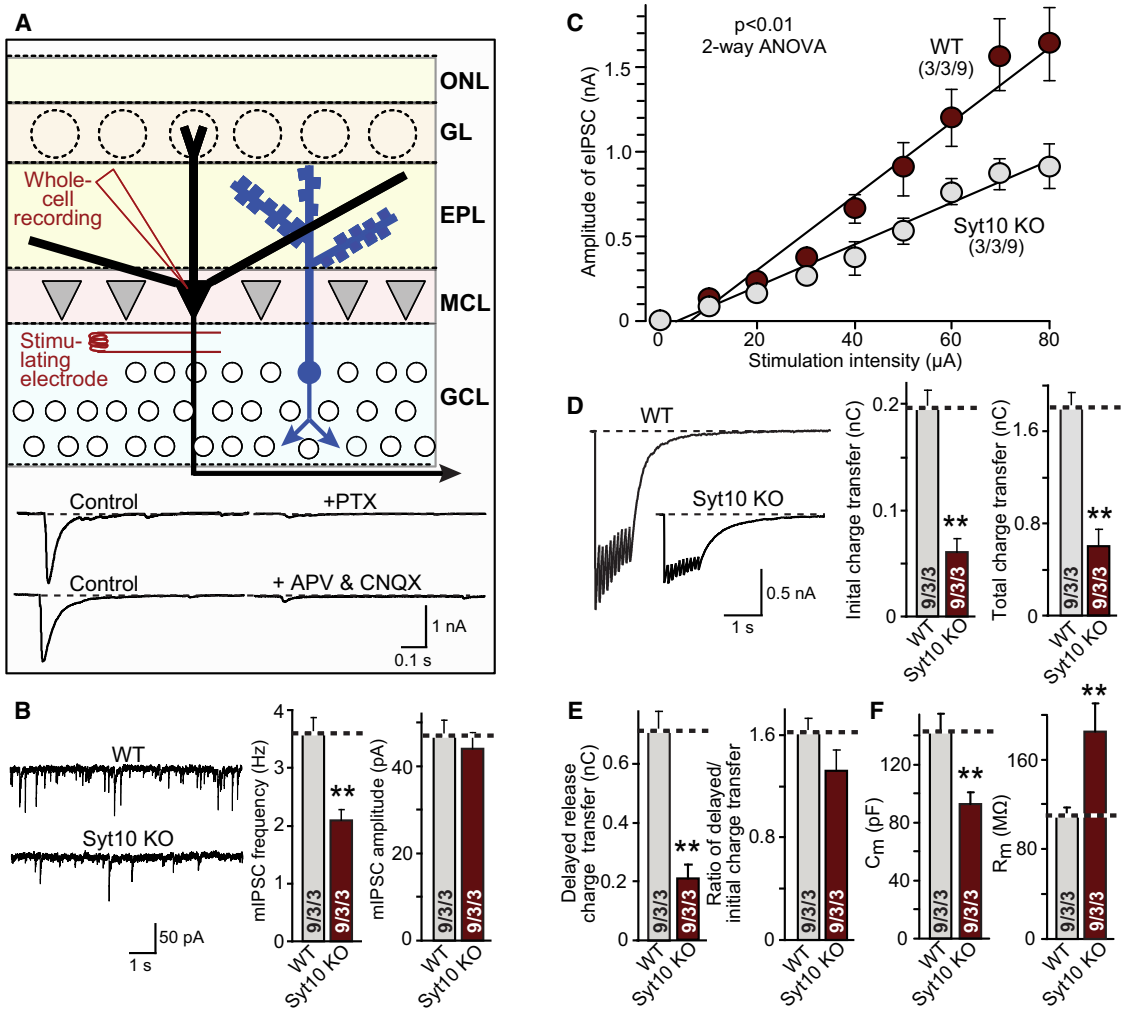

Figure 2. Syt10 KO Impairs Synaptic Transmission as Analyzed in Acute Olfactory Bulb Slices

(A) Recording strategy. Whole-cell recordings were performed in mitral neurons; inhibitory postsynaptic currents (IPSCs) were triggered by stimulation (80 μA for 1 s) with an extracellular concentric bipolar electrode in the granule cell layer to antidromically activate mitral neurons. IPSCs are dependent on retrograde action potentials in mitral neurons that trigger reciprocal excitatory postsynaptic currents (EPSCs) and IPSCs in dendro-dendritic synapses in the external plexiform layer (EPL), as shown by the sensitivity of responses to both the GABA-receptor blocker picrotoxin (PTX) and the glutamate receptor blockers D-APV and CNQX (bottom). EPSCs are not visible in the mitral cell recordings because excitatory synapses are only formed on granule cells, not between mitral cells. For optimization of the location of stimulus electrodes, see Figure S2A (ONL, olfactory nerve layer; GL, glomerular layer; MCL, mitral cell layer; GCL, granule cell layer).

(B) Representative traces (left), frequency (middle) and amplitude (right) of spontaneous 'mini' mIPSCs recorded in 1 μM tetrodotoxin (TTX), 20 μM CNQX, and 50 μM D-APV.

(C) Input/output curves of evoked IPSCs (for sample traces, see Figure S2B).

(D) Representative traces (left) and synaptic charge transfer during the initial 100 ms (middle) and total train (right) of evoked IPSCs elicited by a 10 Hz stimulus train at 80 μA applied for 1 s.

(E) Analysis of delayed release during the 10 Hz 1 s stimulus train as the delayed charge transfer (left) and the ratio of delayed to total charge transfer (right).

(F) Capacitance (left) and input resistance (right) of mitral cells in olfactory bulb slices from wild-type and Syt10 KO mice.

All summary graphs show means ± SEMs; number of recordings/slices/animals analyzed are shown in individual bars. Statistical analyses were performed by Student's t test comparing mitral cell neurons in Syt10 KO and littermate wild-type control slices (** = $p < 0.01$), except for the input/output cure which was analyzed by 2-way ANOVA ($F = 12.84$). See also Table S1.

Figure 2A). Retrograde action potentials in mitral neurons trigger excitation of granule neuron dendrites, which then elicit inhibitory GABAergic postsynaptic currents (IPSCs) that can be monitored in the mitral neurons. Optimization experiments revealed that these events are best induced by stimulating close to the mitral cell layer (Figure S2A). The nature of the IPSCs thus observed was validated by the demonstration that they are blocked both by inhibitors of inhibitory and of excitatory transmission (Figure 2A).

In mitral cells from Syt10 KO mice the frequency but not amplitude of spontaneous mIPSCs was decreased ~40% compared to littermate wild-type controls (Figure 2B). Input/output

curves uncovered a significant decrease in synaptic strength (Figures 2C and S2B). IPSCs measured during a 10 Hz stimulus train applied for 1 s were uniformly decreased ~70%; this decrease was equally observed for the first response and for delayed release, a form of asynchronous release (Maximov and Südhof, 2005), suggesting that the synaptic change consisted in an overall decrease in synaptic transmission capacity, not in an impairment of a particular type of release (Figures 2D and 2E). Moreover, total neuronal cell capacitance was decreased ~30%, whereas the input resistance was increased ~75%, indicating that Syt10 KO neurons are smaller and electrically 'tighter' (Figure 2F).

Syt10 KO Decreases Excitatory and Inhibitory Synaptic Responses in Cultured Olfactory Bulb Neurons

Our electrophysiological experiments in acute slices suggest that deletion of Syt10 impairs synaptic transmission in the olfactory bulb, but do not reveal whether excitatory and/or inhibitory synapses are affected. To measure synaptic transmission more directly, we examined cultured olfactory bulb neurons from conditional (floxed) Syt10 KO mice. Neurons were infected with lentiviruses expressing inactive cre recombinase (as a control), or active cre recombinase (to induce acute deletion of Syt10; Figure 1A; Ho et al., 2006). In this manner, we analyzed identical populations of neurons that only differ in the expression of inactive versus active cre recombinase. Moreover, we additionally examined Syt1 KO neurons to test whether Syt1 and Syt10 perform similar functions (Figure 3).

Inspection of cultured olfactory bulb neurons identified two predominant types of neurons, large (~27 μm diameter) and small neurons (~12 μm diameter). As shown below, these neurons likely represent mitral/tufted neurons and granule cells, respectively, with the latter also including other, less abundant types of interneurons (Trombley and Westbrook [1990]). In the following, we recorded IPSCs and EPSCs from presumptive mitral neurons, and additionally EPSCs from granule neurons.

The phenotype produced by the acute deletion of Syt10 was identical for excitatory and inhibitory synaptic transmission in both types of neurons, as far measured: spontaneous 'mini' frequencies were decreased 30%–50% without a change in mini amplitude, the amplitudes of responses triggered by action potentials were decreased ~40%, and release induced by hypertonic sucrose (Rosenmund and Stevens, 1996) was lowered by ~50% (Figures 3A-3L). Thus, the Syt10 KO uniformly causes a loss of overall synaptic strength in excitatory and inhibitory synapses in mitral and granule cell neurons.

Direct comparisons of the Syt10 KO phenotype with that of the Syt1 KO, analyzed in parallel in the same preparation, revealed that the two synaptotagmin KOs caused completely different effects. Specifically, whereas the Syt10 KO decreased the mini mIPSC frequency in mitral neurons ~50%, the Syt1 KO increased it ~300% (Figures 3I and 3J); whereas the Syt10 KO decreased the amplitude of evoked IPSCs ~40%, the Syt1 KO decreased it > 90% (Figure 3K); and finally, whereas the Syt10 KO decreased synaptic transmission induced by hypertonic sucrose ~50%, the Syt1 KO had no effect on this type of synaptic response (Figure 3L). These results show that Syt10 operates in a different pathway or by a different mechanism than Syt1.

Syt10 KO Decreases the Size and Dendritic Arborization of Olfactory Bulb Neurons, but Not the Synapse Density per Dendritic Length

The physiological phenotype of Syt10 KO neurons could be explained by a uniform decrease in the strength of all synapses, or by a decrease in synapse numbers. Moreover, the slice recordings revealed that the Syt10 KO caused a significant decrease in capacitance and increase in input resistance in mitral neurons (Figure 2F). Strikingly, we observed the same effect of the Syt10 KO in cultured mitral and granule cell neurons, whereas in parallel experiments the Syt1 KO produced no change in these parameters (Figures 4A and 4B). These results suggest that the Syt10 KO phenotype may be due, at least in part, to a decrease in neuronal size.

To test this hypothesis, we stained cultured olfactory bulb neurons with vGlut1 antibodies and measured the sizes of the cell bodies of excitatory vGlut1-positive neurons (presumably primarily mitral cells), and of inhibitory vGlut1-negative neurons (presumably primarily granule cells). These measurements confirmed that the excitatory neurons were twice as large as inhibitory neurons (Figures 4C and 4D), validating the size classification used for the electrophysiological experiments (Figure 3). Moreover, these measurements revealed that the Syt10 KO significantly reduced the size of both types of neurons (Figures 4C and 4D), confirming the hypothesis from the capacitance measurements that the Syt10 KO decreases the neuronal soma size (Figure 4A).

To examine whether not only the neuronal cell bodies, but also the entire neuronal arborization is affected by the Syt10 KO, we expressed tdTomato in a small subset of neurons by transfection, and measured the total length and branching complexity of their dendrites (Figures 4E–4G). Strikingly, the Syt10 KO decreased the total dendritic length of mitral neurons by ~40% (Figure 4F), and reduced their arborization even more (Figure 4G). In contrast, measurements of the density of synapses per dendritic length uncovered no change (Figures 4H and 4I). Viewed together, these data show that the Syt10 KO causes a general decrease in neuronal size and arborization in olfactory bulb neurons, resulting in a decrease in the number of synapses per neuron even though synapse density per dendrite length is unchanged. These findings in cultured neurons agree well with those of the olfactory bulb sections (Figures 1C-1F), and the ~40% decrease in neuronal size and dendritic length corresponds closely to the impairment in synaptic strength we observed electrophysiologically (Figure 2 and Figure 3).

Syt10 Function Is Not Redundant with that of Closely Related Syt3, Syt5, or Syt6, and Requires Ca^{2+} Binding to its C_2 Domains

Syt10 belongs to a group of Ca^{2+}-binding synaptotagmins that includes Syt3, Syt5, and Syt6, and that differs from the group containing Syt1. The Syt10 group of synaptotagmins exhibit a high degree of sequence homology, and may heterodimerize (Fukuda et al., 1999), suggesting that these synaptotagmins are functionally redundant, similar to the redundancy among

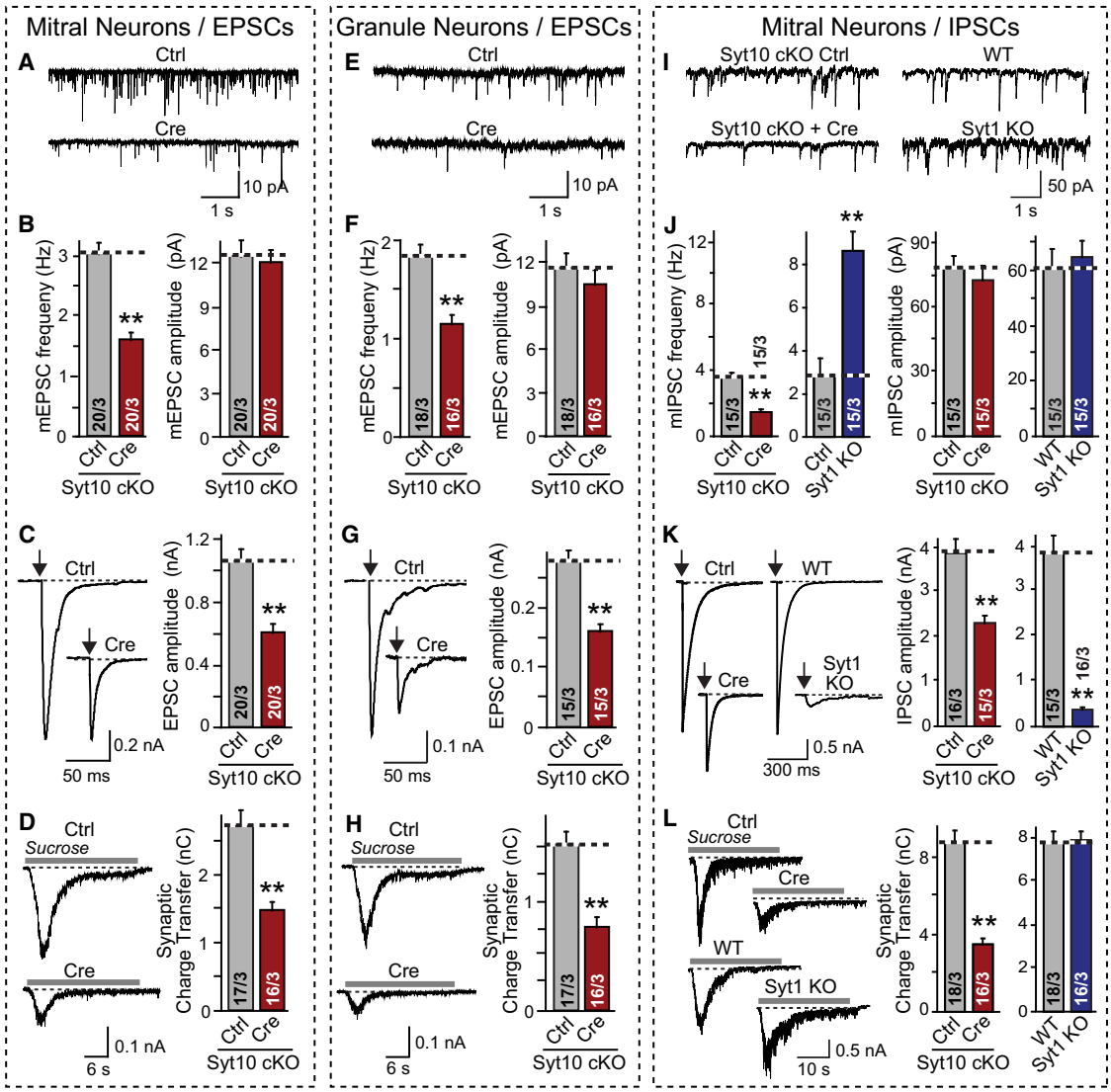

Figure 3. Conditional Syt10 KO Decreases Synaptic Strength as Analyzed in Cultured Olfactory Bulb Neurons

Olfactory bulb neurons were cultured from conditional Syt10 KO mice (Syt10 cKO), infected at DIV2-3 with lentiviruses expressing inactive (Ctrl) or active Cre recombinase (Cre) for acute deletion of Syt10, and analyzed on DIV14-16 by whole-cell patch-clamp recordings from large (primarily mitral cells, [A–D] and [I–L]) or small neurons (primarily granule cells, [E–H]; for validation of neuronal types, see Figure 4). Excitatory (A–H) and inhibitory synaptic responses (I–L) were recorded in 50 μM picrotoxin or 20 μM CNQX and 50 μM D-APV, respectively. Parallel experiments were performed with mitral neurons cultured from littermate wild-type (WT) and Syt1 KO mice as shown in panels (I)–(L).

(A and B) Representative traces (top) and summary graphs of the frequency and amplitude (bottom) of spontaneous "mini" exitatory mEPSCs recorded in 1 μM tetrodotoxin in mitral neurons (red = Syt10 KO; blue = Syt1 KO).

(C) Representative traces (left) and summary graphs of the amplitudes of evoked EPSCs (arrows, action potential).

(D) Representative traces (left) and summary graphs of the total charge transfer (right) of EPSCs evoked by application of 0.5 M sucrose (gray line) in 1 μM TTX.

(E–H) Same as A-D, except that excitatory synaptic responses were analyzed in granule cell neurons.

(I–L) Same as A-D, except that inhibitory synaptic responses were analyzed in mitral cell neurons, and Syt1 KO neurons were analyzed in parallel.

All summary graphs show means ± SEMs; number of cells/number of independent cultures analyzed are shown in individual bars. Statistical analyses were performed by Student's t test comparing the cre-recombinase treated and control neurons (**$p < 0.01$). See also Table S1.

the Syt1 group of synaptotagmins that act as Ca^{2+}-sensors for fast synaptic vesicle exocytosis (Xu et al., 2007). To test this hypothesis, we examined whether the Syt10 KO phenotype, measured electrophysiologically, could be rescued by other members of its group of synaptotagmins. Unexpectedly, we found that only expression of Syt10, but not of Syt3, Syt5, or Syt6, reversed the decrease in synaptic strength, the decline in cell capacitance, and the increase in input resistance produced by the Syt10 KO (Figures 5A–5C).

We next probed whether Syt10 acts functionally as a Ca^{2+}-sensor by mutating the Ca^{2+}-binding sites of its C_2-domains (Figure S3B; Shin et al., 2009). Rescue experiments showed that the

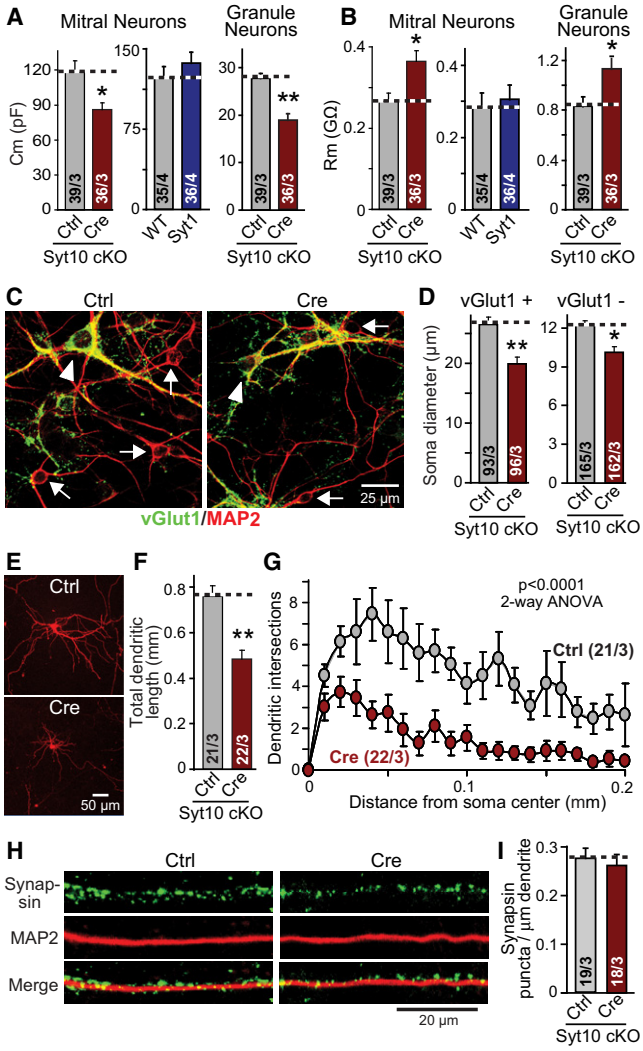

Figure 4. Syt10 KO Decreases Neuronal Size and Arborization but Not Synapse Density per Dendritic Segment

Olfactory bulb neurons were cultured as described for Figure 3.

(A and B) Capacitance (Cm) and input resistance (Rm) measurements from mitral and granule cell neurons of Syt10 and Syt1 KO neurons compared to controls.

(C) Representative images of control and cre-recombinase expressing conditional Syt10 KO neurons stained for the excitatory marker vGlut1 (green), and the neuronal marker MAP2 (red; yellow = overlap; arrowhead = vGlut1 positive cell bodies; arrows = vGlut1 negative cell bodies).

(D) Size of the soma of neurons expressing (vGlut1+) or lacking the excitatory marker vGlut1 (vGlut1-), to identify the former as the larger mitral and tufted neurons, and the latter as primarily composed of the smaller granule cell neurons.

(E–G) Representative images of mitral neurons expressing tdTomato (introduced by transfection at DIV7; E); measurements of the total dendritic length of such neurons (F); and Sholl analysis of dendritic branching of these neurons (G).

(H and I) Representative immunofluorescence images of the dendrites of mitral neurons (left), and summary graph of the synapse density on such dendrites (right). Cultured olfactory bulb neurons were stained for MAP2 and synapsin, and the synapse density on representative dendritic sections was quantified. Summary graphs depict means ± SEMs; number of cells/independent cultures analyzed are shown in individual bars. Statistical analyses for summary graphs were performed by Student's t test comparing the cre-recombinase treated neurons to control neurons (*$p < 0.05$; **$p < 0.01$), except for (G), which was assessed by 2-way ANOVA. See also Table S1.

Ca^{2+}-binding site mutation inactivated the ability of Syt10 to reverse the Syt10 KO phenotype (Figures 5D-5F). Thus, Syt10 acts as a Ca^{2+}-sensor to maintain the normal size and arborization of olfactory bulb neurons, with a function that is unique to this synaptotagmin isoform and not shared by other, closely related synaptotagmins.

Syt10 KO Decreases IGF-1 Secretion

How does Syt10 regulate the growth and arborization of olfactory bulb neurons? Since the experiments up to now indicate that Syt10 might be a Ca^{2+}-sensor for the exocytosis of an unknown growth factor, we tested whether cultured olfactory bulb neurons exhibit an activity-dependent trophic phenotype. At the same time, we examined whether olfactory bulb neurons secrete IGF-1 in an activity-dependent manner, because this growth factor is abundantly expressed in olfactory bulb neurons, supports olfactory bulb neurogenesis and differentiation, and maintains olfactory map formation (Bartlett et al., 1991; Giacobini et al., 1995; Vicario-Abejon et al., 2003; Cheng et al., 2003; Scolnick et al., 2008).

Chronic treatment of cultured wild-type olfactory bulb neurons with 1 µM tetrodotoxin (TTX), a Na^+-channel blocker that silences network activity in cultured neurons, caused a decrease in cell capacitance and an increase in input resistance similar to the effect of the Syt10 KO (Figure S3D). Direct measurements of the IGF-1 concentration in the medium revealed a significant decrease of secreted IGF-1 in TTX-treated neurons (Figure S3D). Thus, silencing of olfactory bulb neurons stunts their growth, and decreases IGF-1 secretion.

We next tested whether secretion of IGF-1 could be stimulated by mild depolarization of cultured olfactory bulb neurons by incubating them in 15 mM K^+, and whether the Syt10 KO impaired the stimulated secretion of IGF-1 (Figures 5G–5I). Indeed, 15 mM K^+ depolarization massively stimulated IGF-1 secretion; this increase was significantly decreased by the Syt10 KO, whereas the baseline secretion of IGF-1 was unaffected (Figures 5G–5I). We performed these experiments at two different ages of the neuronal cultures (DIV7 and DIV14) to ensure that the observed effects were stable, and obtained similar results (Figures 5G and 5H). The Syt10 KO phenotype was rescued by wild-type Syt10, whereas mutant Syt10 unable to bind Ca^{2+} was also unable to rescue the phenotype. Morever, we tested the effect of the Syt1 KO on K^+-stimulated IGF-1 secretion but found no change, confirming the specificity of the Syt10 KO phenotype (Figure 5I).

Exogenous IGF-1 Rescues the Syt10 KO Phenotype

The selective effect of the Syt10 KO on IGF-1 secretion, and its rescue by wild-type but not mutant Syt10, correlates well with the overall Syt10 KO phenotype. However, the fact that the Syt10 KO only partially suppresses stimulated secretion of IGF-1 (Figures 5G and 5H) raises the question whether the Syt10 KO phenotype is entirely due to a relative lack of IGF-1 secretion,

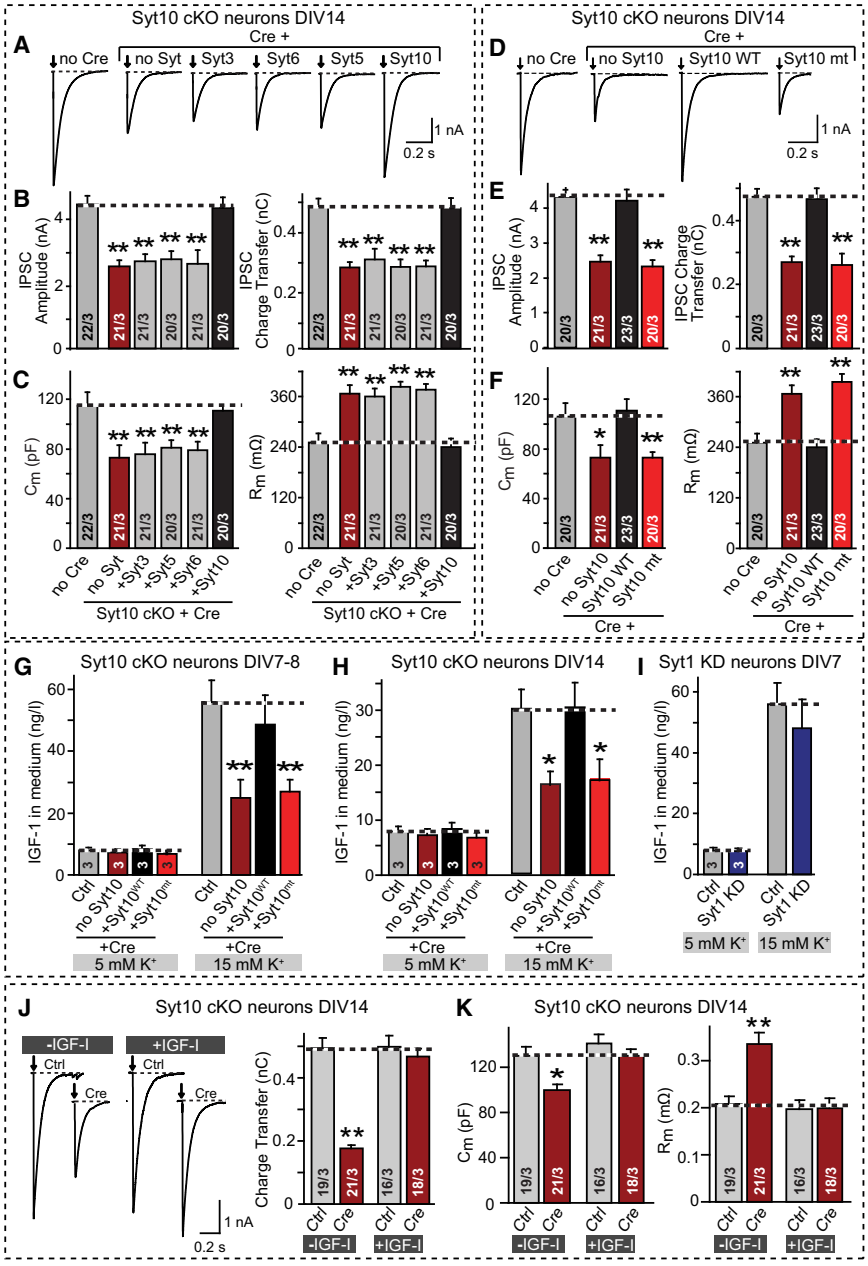

Figure 5. Syt10 Functions as a Specific Ca^{2+}-Sensor for IGF-1 Secretion in Cultured Olfactory Bulb Neurons

(A–C) Only Syt10 but not closely related synaptotagmin isoforms (Syt3, Syt5, and Syt6) rescue the Syt10 KO phenotype. Olfactory bulb neurons cultured from conditional Syt10 KO mice (Syt10 cKO) were infected with control (Ctrl) or Cre-recombinase expressing lentiviruses (Cre) that coexpress the indicated synaptotagmins. Panels depict representative traces of evoked IPSCs (A) and summary graphs of the amplitude ([B] left) and charge transfer of evoked IPSCs ([B] right), and of the capacitance ([C] left) and input resistance ([C] right) monitored in mitral neurons (see also Figure S3A).

(D–F) Same as A-C, except that neurons were rescued with wild-type ($Syt10^{WT}$) or mutant Syt10 in which the Ca^{2+}-binding sites of both C_2-domains were abolished ($Syt10^{mt}$). For a description of the mutation, see Figure S3B.

(G and H) Measurements of depolarization-induced IGF-1 secretion by cultured olfactory bulb neurons after stimulation with 5 or 15 mM K^+ for 1 hr at DIV7-8 (G) or DIV14 (H). Neurons cultured from conditional Syt10 KO mice were infected with lentiviruses expressing inactive (Ctrl) or active cre-recombinase (Cre), the latter without (no Syt10) or with coexpression of wild-type ($Syt10^{WT}$) or Ca^{2+}-binding site mutant Syt10 ($Syt10^{mt}$). The IGF-1 concentration in the medium was measured by ELISA. Note that the secretory capacity decreases with the age of the culture, but the effect of the Syt10 KO remains the same. (see Figure S3C for ELISA standardization).

(I) Same as G and H, except that wild-type olfactory bulb neurons without or with shRNA-dependent knockdown of Syt1 (Syt1 KD) were analyzed.

(J) Representative traces (left; arrows = action potentials) and summary graphs of the charge transfer (right) of IPSCs monitored in mitral neurons from conditional Syt10 KO mice that were infected with control (Ctrl) or cre-recombinase-expressing lentivirus (Cre) at DIV2, and maintained in the absence or presence of 50 μg/l synthetic IGF-1 (~6.5 nM) added to the medium from DIV7 onward (see Figure S3E for IPSC amplitudes).

(K) Summary graphs of the the neuronal capacitance (left) and input resistance (right) of mitral neurons treated as described in J.

All summary graphs depict means ± SEMs; number of cells and number of independent cultures analyzed is shown in individual bars except for G-I, in which the number of independent culture experiments is indicated in the bars. Statistical analyses were performed by Student's t test comparing the cre-recombinase treated neurons to control neurons (*$p < 0.05$; **$p < 0.01$). See also Table S1.

or whether additional factors contribute. To address this question, we tested whether the Syt10 KO phenotype can be rescued by simple addition of exogenous IGF-1 to the culture medium.

Strikingly, supplementation of the culture medium with synthetic IGF-1 from DIV7 onward completely reversed the Syt10 KO phenotype, but had no effect on the properties of control neurons (Figures 5J and 5K). Thus, a relative lack of IGF-1 secretion fully accounts for the overall Syt10 KO phenotype.

Syt10 and IGF-1 Colocalize in Somatic and Dendritic Vesicles in Mitral Neurons

To localize Syt10 and IGF-1 in neurons, we tested available antibodies (commercial and lab-made antibodies) with various protocols, but obtained no specific immunocytochemical signals. Therefore, we employed exogenously expressed, tagged Syt10 and IGF-1 for localization studies. We generated an N-terminal fusion protein of Syt10 with pHluorin (Miesenböck

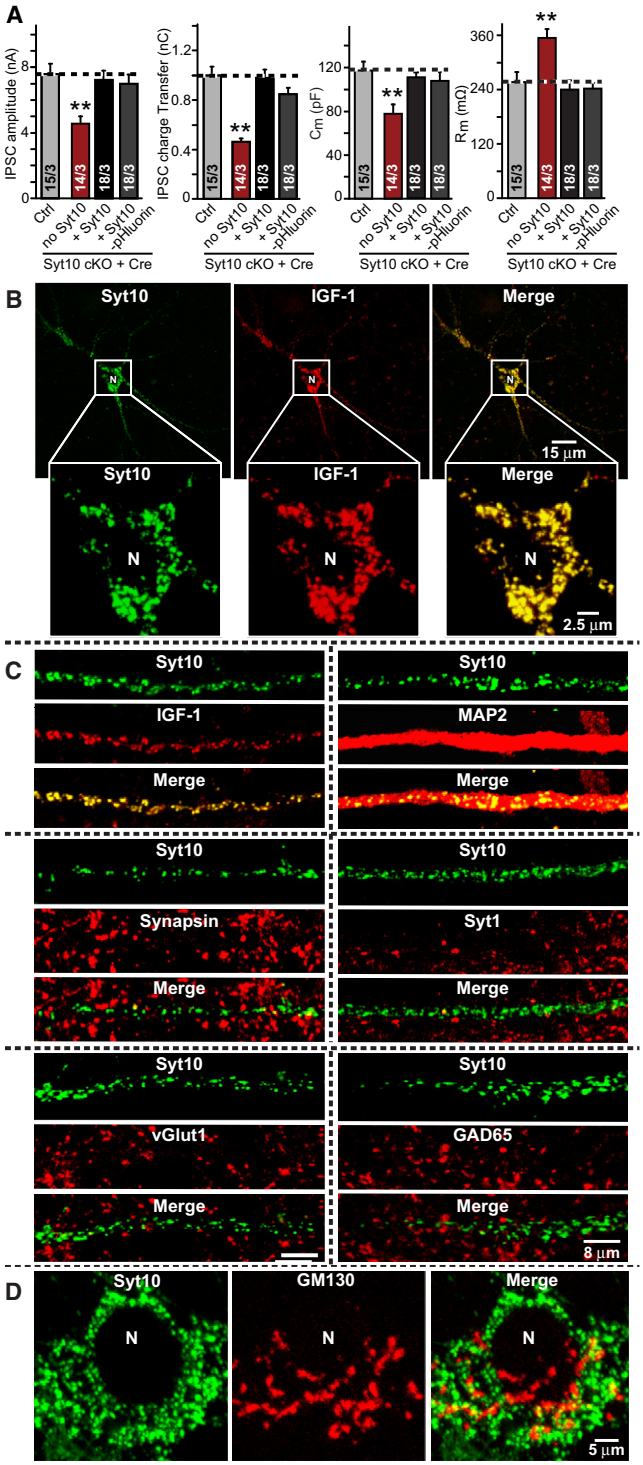

Figure 6. Colocalization of Syt10 and IGF-1 in Olfactory Bulb Neurons

(A) pHluorin-tagged Syt10 rescues the decrease in total synaptic transmission induced by Syt10KO. Summary graphs show the IPSC amplitude (left), IPSC charge transfer (left middle), capacitance (right middle), and input resistance (right) monitored in mitral neurons from conditional KO mice infected either with control lentivirus (Ctrl) or with lentivirus expressing cre recombinase alone (no Syt) or together with untagged Syt10 or with pHluorin-tagged Syt10. Data depict means ± SEMs; number of cells and number of independent cultures analyzed is shown in individual bars. Statistical analyses were performed by Student's t test comparing the cre-recombinase treated neurons to control neurons (** = $p < 0.01$).

(B) Low- and high-magnification images of a neuron with lentivirally expressed Syt10-pHluorin and transfected Flag-tagged IGF-1, analyzed by indirect immunofluorescence. Note complete colocalization of Syt10 and IGF-1. For demonstration that Flag-tagged IGF-1 is secreted and for an analysis of the size of the vesicles positive for Syt10 and IGF-1, see Figure S5.

(C) Analysis of the dendritic localization of Syt10 in comparison with a series of pre- and postsynaptic markers. Note the completely dendritic localization of Syt10.

(D) Relative localization of Syt10 and of the Golgi-marker GM130 in the soma of a neuron to illustrate that Syt10 is not part of the Golgi apparatus. See also Table S1.

et al., 1998) to allow visualization of Syt10 trafficking in neurons, and added a Flag-epitope to IGF-1. Flag-tagged IGF-1 was secreted similar to endogenous IGF-1 (Figure S4A), and pHluorin-tagged Syt10 fully rescued the Syt10 KO phenotype, suggesting that it is fully functional (Figure 6A).

We next analyzed by immunofluorescence labeling the location of IGF-1 and Syt10 in neurons expressing the tagged proteins. Strikingly, the two proteins completely colocalized, but their locations did not overlap with those of synaptic markers (Figures 6B–6D). Specifically, both Syt10 and IGF-1 were found in cytoplasmic vesicles (estimated size: Syt10-pHluorin vesicles = 0.99 ± 0.06 μm^2; Flag-IGF-1 vesicles = 1.02 ± 0.06 μm^2; n = 3 independent cultures; Figure S4B) that were abundantly present in the soma of neurons (Figure 6B) as well as all their dendrites (Figure 6C). These vesicles did not colocalize with any synaptic vesicle protein analyzed (Figure 6C), or with the Golgi marker GM130 (Figure 6D). Thus, Syt10 is present on neuronal vesicles containing IGF-1 that are not enriched at synapses.

Neuronal Depolarization Induces Rapid Exocytosis of Syt10-Containing Vesicles

pHluorin fluorescence is quenched at acidic pH, but activated at neutral pH (Miesenböck et al., 1998); thus, the pHluorin moiety on tagged Syt10 (Figure 6) allows imaging of Syt10 trafficking in and out of acidic compartments, such as intracellular vesicles. We found that under resting conditions, neurons expressing pHluorin-tagged Syt10 exhibited very weak fluorescence, suggesting that the pHluorin tag was localized inside an acidic vesicle lumen (Figure 7A). Consistent with this notion, addition of NH_4Cl that rapidly neutralizes the pH of intracellular organelles caused a robust increase in Syt10-pHluorin fluorescence (Figure 7A). The effect of NH_4Cl was rapidly reversed by washing NH_4Cl out. This allowed us to visualize the Ca^{2+}-dependent trafficking of individual Syt10-positive vesicles in neurons. We added and washed out NH_4Cl to identify the vesicles, and subsequently tested whether the same vesicles could be stimulated to undergo exocytosis by K^+-induced depolarization (Figure 7A).

We treated neurons expressing Syt10-pHluorin with NH_4Cl, imaged the increase in pHluorin fluorescence, washed out the NH_4Cl, and then imaged Syt10-pHluorin fluorescence after application of 15 mM K^+, a stimulus that induced IGF-1 secretion as described above (Figures 5G–5I). Strikingly, depolarization of

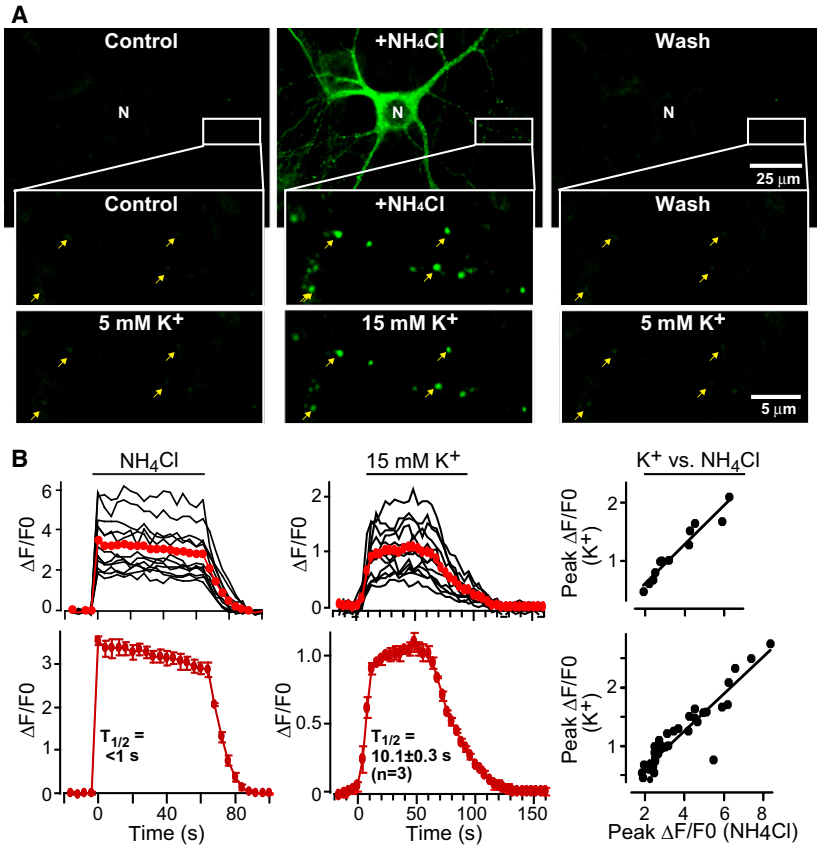

Figure 7. Monitoring Activity-Dependent Exo- and Endocytosis of pHluorin-Tagged Syt10

(A) Syt10-pHluorin signal in a representative neuron expressing Syt10-pHluorin that was first incubated with 50 mM NH_4Cl to neutralize all intracellular acidic compartments, thereby visualizing pHluorin-containing compartments, and washed afterwards with Tyrode's solution. The same neuron was subsequently stimulated with 15 mM K^+ to trigger Ca^{2+}-dependent vesicle exocytosis as shown in the bottom images, and washed again (arrows, example vesicles). (B) Quantitation of the pHluorin signal observed in neurons during sequential exposure to 50 mM NH_4Cl or 15 mM K^+. Traces from an exemplary neuron repeatedly imaged are shown on top (average signals from the exemplary traces are shown in red), and summary graphs for multiple neurons (means ± SEMs; n = 3 independent cultures) are shown on the bottom. The graphs on the right depict the correlation between fluorescent changes evoked by K^+ and NH_4Cl in the same neurons. See also Table S1.

neurons with 15 mM K^+ caused a similar pattern of vesicular pHluorin fluorescence activation as a prior NH_4Cl exposure (Figure 7A). These data support the conclusion of the IGF-1 secretion and the Syt10 and IGF-1 localization experiments that Ca^{2+}-binding to Syt10 present on IGF-1 containing vesicles triggers their exocytosis.

To quantify the dynamics of Syt10-mediated exocytosis, we measured the time course of the pHluorin-signal in neurons after addition of NH_4Cl or K^+ (Figure 7B). On average, 15 mM K^+ produced ~30% of the total pHluorin-fluorescence increase revealed by NH_4Cl, suggesting that approximately a third of the Syt10-containing vesicles were stimulated for exocytosis by 15 mM K^+. The time course of K^+-stimulated exocytosis was rapid (~10 s; Figure 7B). Although the extent of fluorescence increase induced by NH_4Cl and K^+ varied between neurons, they correlated well with each other within the same neuron (Figure 7B). Thus, Syt10 is a vesicular Ca^{2+}-sensor for IGF-1 containing vesicles that mediates rapid activity-dependent secretion of IGF-1.

DISCUSSION

Synaptotagmins function as major Ca^{2+}-sensors for exocytosis (Gustavsson and Han, 2009; Südhof and Rothman, 2009). Eight Ca^{2+}-binding synaptotagmins are expressed in brain, but only Syt1, Syt2, Syt7, and Syt9 have a known biological role, namely a largely overlapping function as Ca^{2+}-sensors for synaptic and neuroendocrine vesicle exocytosis (Geppert et al., 1994; Fukuda et al., 2002; Pang et al., 2006; Sorensen et al., 2003; Lynch and Martin, 2007; Xu et al., 2007; Gustavsson et al., 2008 and 2009; Schonn et al., 2008). The remaining four Ca^{2+}-binding synaptotagmins (Syt3, Syt5, Syt6, and Syt10) constitute a separate homologous group, united by common Ca^{2+}-binding features of their C_2-domains (Sugita et al., 2002), and by similar intravesicular N-terminal sequences that form disulfide-bonded dimers (Fukuda et al., 1999). Despite their abundant neuronal expression, however, no function is known for these synaptotagmins in neurons. Here, we have analyzed the role of one member of this class of synaptotagmins, Syt10, focusing on the olfactory bulb where this protein is expressed at high levels (Mittelstaedt et al., 2009).

We generated conditional and constitutive Syt10 KO mice, and demonstrated that these mice exhibited impaired food-finding behaviors and an overall decrease in synapse numbers in the external plexiform layer, but not the glomerular layer, of the olfactory bulb (Figure 1). We showed that overall synaptic transmission between granule and mitral cell neurons was decreased in acute olfactory bulb slices derived from constitutive Syt10 KO mice, and that both excitatory and inhibitory synaptic strength were lowered in cultured olfactory bulb neurons after conditional deletion of Syt10 (Figure 2 and Figure 3). Strikingly, these changes were accompanied by a decrease in the capacitance and an increase in the input resistance of olfactory bulb neurons, by a decrease in their soma size, and a loss of dendritic arborization, without a change in synapse

density per dendrite length (Figure 2 and Figure 4). The reduction of neuronal size and dendritic branching in Syt10-deficient neurons corresponded to the decrease in synaptic strength in these neurons, suggesting that the Syt10 KO produced an overall loss of synapse numbers between granule and mitral cell neurons due to decreased arborization. Parallel experiments in olfactory bulb neurons lacking Syt1, which belongs to a different group of synaptotagmins and acts as the Ca^{2+}-sensor for fast exocytosis of neurotransmitter vesicles in the same neurons, showed that although the Syt1 KO caused a massive synaptic phenotype in these neurons as expected (Geppert et al., 1994), its phenotype was dramatically different from that of the Syt10 KO in every parameter examined (Figure 3 and Figure 4). Thus, Syt10 and Syt1 perform distinct functions in the same neurons. Moreover, rescue experiments surprisingly revealed that the Syt10 KO phenotype is only rescued by Syt10 but not by other closely related synaptotagmins, indicating that the function of Syt10 is unique and specific (Figure 5). In addition, mutant Syt10 unable to bind Ca^{2+} did not rescue the KO phenotype, suggesting that Syt10 acts as a Ca^{2+}-sensor (Figure 5).

The electrophysiological Syt10 KO phenotype suggested that Syt10 is essential for the activity-dependent secretion of a growth factor in olfactory bulb neurons, prompting us to focus on IGF-1 that is abundantly expressed in olfactory bulb (Aguado et al., 1993; Rotwein et al., 1988) and is essential for olfactory bulb development (Giacobini et al., 1995; Cheng et al., 2003; Scolnick et al., 2008). We thus tested whether IGF-1 is released from olfactory bulb neurons in an activity-dependent manner. Indeed, we found that chronic inactivity impaired IGF-1 secretion in wild-type olfactory bulb neurons, and that acute mild K^+-induced depolarization stimulated IGF-1 secretion from these neurons (Figures 5G–5I and Figure S3D). The Syt10 KO impaired the depolarization-induced stimulation of IGF-1 secretion from olfactory bulb neurons; this impairment could be rescued by wild-type but not by Ca^{2+}-binding site mutant Syt10 (Figures 5D–5F). Importantly, the entire Syt10 KO phenotype could be rescued by simple addition of exogenous IGF-1 to the medium, confirming that a relative loss of IGF-1 secretion fully accounts for the Syt10 KO phenotype (Figures 5J and 5K). Moreover, immunocytochemical experiments revealed that Syt10 and IGF-1 colocalize to an abundant set of cytoplasmic vesicles of $\sim$1 μM diameter that were distributed throughout the cell body and dendrites of the neurons (Figure 6). Finally, using pHluorin-tagged Syt10 we showed that unlike presynaptic neurotransmitter vesicles, Syt10-containing vesicles were somatodendritic, and were triggered for rapid exocytosis by the same mild depolarization used for the IGF-1 secretion stimulation (Figure 7).

We believe our data allow four conclusions. First, they reveal that Syt10 functions as a Ca^{2+}-sensor for exocytosis for a non-synaptic type of vesicles. With this finding, we broaden the synaptotagmin paradigm to other forms of synaptotagmins and other pathways of secretion in neurons, beyond the previously established role of Syt1, Syt2, Syt7, and Syt9 in neurotransmitter and neuropeptide exocytosis (Südhof and Rothman, 2009). Syt10 belongs to a class of Ca^{2+}-binding synaptotagmins that also includes Syt3, Syt5, and Syt6, and that are characterized by N-terminal disulfide bonds that dimerize these synaptotagmins. It had been suggested that these synaptotagmins may function as Ca^{2+}-sensors for exocytosis, possibly even for asynchronous release (Li et al., 1995b; Hui et al., 2005), but no previous demonstration of such a function was possible due to a lack of genetics. Our data confirm that at least one member of this family is indeed a Ca^{2+}-sensor for exocytosis, although not for asynchronous exocytosis of neurotransmitter vesicles, but for a completely different type of vesicle exocytosis in the same neurons that use the Syt1-class of synaptotagmins for neurotransmitter release. Moreover, our data show that Syt10 is not functionally redundant with other members of its class, a surprising finding given suggestions that the synaptotagmins of this class may even heterodimerize (Fukuda et al., 1999).

Second, our data show that two different synaptotagmins control two different Ca^{2+}-dependent secretory pathways in the same neuron. Thus, different synapotagmins specify different secretory pathways. Previous studies have suggested that Syt7 in fibroblasts controls lysosome exocytosis (e.g., see Martinez et al., 2000; Flannery et al., 2010), but in neuroendocrine cells, Syt7 appears to control the same pathway as Syt1, Syt2, and Syt9, and does not regulate a distinct lysosome secretion pathway (Wang et al., 2005; Schonn et al., 2008; Gustavsson et al., 2008 and 2009; Li et al., 2009). The finding that two different synaptotagmins control exocytosis of two non-overlapping secretory pathways, despite a similar Ca^{2+}-binding mechanism, opens up the possibility that the many different synaptotagmins which have been described molecularly but remain to be characterized functionally may be involved in controlling distinct secretory pathways in neurons. Thus, synaptotagmins may embody specificity signals that direct regulation of different pathways in a pathway-specific manner.

Third, our data uncover, to our knowledge, the first regulatory mechanism for IGF-1 secretion. Although IGF-1 is an important and widely studied growth factor with many essential functions, little is known about how it is secreted and how its secretion is regulated. Our data show that at least in olfactory bulb neurons, IGF-1 is secreted by an activity-dependent, Ca^{2+}-regulated vesicular pathway of exocytosis.

Finally, our results provide mechanistic insights into the molecular and physiological basis of activity-dependent neural circuit development in the olfactory bulb. Previous studies have shown that neuronal activity plays an essential role in the formation and maintenance of olfactory sensory maps. Intriguingly, IGF-1 has also been implicated in shaping the connectivity of developing olfactory neurons (Scolnick et al., 2008). Our results suggest that the activity- and Syt10-dependent vesicular pathway of IGF-1 secretion may play a central role in the activity-dependent tuning of emerging olfactory circuits by mediating IGF-1 release in response to sensory stimuli or spontaneous neuronal firing.

Our results also raise new questions. Clearly, IGF-1 secretion is not universally dependent on Syt10 because the Syt10 KO phenotype does not resemble the IGF-1 KO phenotype (Baker et al., 1993; Liu et al., 1993; Beck et al., 1995). This suggests that IGF-1 secretion mechanisms differ among cell types – for example, it is possible that IGF-1 secretion in other cells involves other types of synaptotagmins (e.g., Syt3, Syt5, or Syt6), or different types of regulation. The Syt10 pathway may have evolved in conjunction with the continuing adult neurogenesis

of granule neurons in the olfactory bulb, but the expression of Syt10 in other brain areas, and the induction of Syt10 expression by seizures (Babity et al., 1997), indicate that the Syt10 pathway may also operate outside of olfactory bulb neurons, and perform a general role in injury responses induced by seizures. Thus, it will be fascinating to test whether seizures initiate expression of a Ca^{2+}- and Syt10-regulated IGF-1 secretory pathway as an injury response. In the olfactory bulb and elsewhere, IGF-1 regulates membrane expansion at the axonal growth cone in a process that is necessary for axon specification (Giacobini et al., 1995; Scolnick et al., 2008), which may also be important for neuronal repair. In addition, IGF-1 promotes dendritic development (Cheng et al., 2003). Furthermore, although our data support the notion that synaptotagmins generally function in regulating exocytosis, they raise the question of the function of the other synaptotagmins – for example, does the adundant expression of all of synaptotagmins in brain mean that they mediate other parallel types of Ca^{2+}-triggered exocytosis, i.e., that neurons can have even more different synaptotagmin-dependent pathways of exocytosis? Finally, it is unclear why Syt10 and the other disulfide-bond dimerized synaptotagmins contain their signature disulfide bonds. Independent of the answers to these questions, however, it seems likely that synaptotagmins generally control secretory pathways by similar molecular mechanisms, and that they do so by isoform-specific interactions that allow independent regulation of multiple Ca^{2+}-triggered pathways in the same cell.

EXPERIMENTAL PROCEDURES

Generation and Husbandry of Mutant Mice

All mice described in this paper are deposited with Jackson Labs, and are freely available. The targeting strategy, primer sequences, mouse breeding procedures, and behavioral tests are described in detail in the extended methods in the SOMs. All analyses in this paper on constitutive KO mice were performed with littermate controls.

Constructs and Lentiviruses

Lentiviruses expressing inactive and active cre-recombinase as EGFP-fusion proteins without or with rescue proteins were produced in transfected HEK293 cells as described (Ho et al., 2006).

Culture of Olfactory Bulb Neurons

Culture of olfactory bulb neurons were obtained using the same protocol as for cortical neurons (Maximov et al., 2007; Xu et al., 2007; Pang et al., 2010).

Morphological Analyses

Morphological analyses were performed on olfactory bulb sections and cultured olfactory neurons as described in detail in the SOMs.

Electrophysiological Analyses

Electrophysiological analyses were performed in acute olfactory bulb slices from 14- to 16-day-old wild-type and Syt10 KO (−/−) mice as described (Chen and Shepherd, 1997), or in olfactory bulb cultured as described above, using the methods we described previously (Maximov et al., 2007; Xu et al., 2007; Pang et al., 2010). For details, see SOMs.

Measurements of IGF-1 Secretion

Syt10- or Syt1-deficient or control cultured olfactory bulb neurons were incubated at DIV7 or DIV14 for 1 hr in 150 μl fresh culture medium containing either 5 mM or 15 mM KCl, with adjusted osmolarity. After stimulation, the IGF-1 concentration in the medium was measured using the Quantikine Mouse/Rat IGF-1 Immunoassay (http://www.rndsystems.com/pdf/mg100.pdf,R&D Systems, Inc.; see Figure S3).

Syt10-pHluorin Live Cell Imaging

Syt10-pHluorin was lentivirally expressed in cultured olfactory bulb neurons at DIV2, and analyzed at DIV14-16 as described in the SOMs.

Statistical Analyses

All experiments were performed in a 'blinded' fashion, i.e., the experimenter was unaware of the genotype of the samples being studied, with at least three independent cultures for each type of experiment. All statistical comparisons were made using Student's t test or 2-way ANOVA as indicated.

SUPPLEMENTAL INFORMATION

Supplemental Information includes Extended Experimental Procedures, four figures, and one table and can be found with this article online at doi:10.1016/j.cell.2011.03.034.

ACKNOWLEDGMENTS

We thank Dr. R.E. Hammer (UT Southwestern, Dallas) for experimental support; Dr. E.R. Barton (U. of Pennsylvania) for providing the IGF-1 cDNA; and Drs. Z.P. Pang and W. Xu for advice and reagents.

Received: May 5, 2010
Revised: December 24, 2010
Accepted: March 7, 2011
Published: April 14, 2011

REFERENCES

Aguado, F., Rodrigo, J., Cacicedo, L., and Mellstrom, B. (1993). Distribution of insulin-like growth factor-I receptor mRNA in rat brain. Regulation in the hypothalamo-neurohypophysial system. J. Mol. Endocrinol. *11*, 231–239.

Babity, J.M., Armstrong, J.N., Plumier, J.C., Currie, R.W., and Robertson, H.A. (1997). A novel seizure-induced synaptotagmin gene identified by differential display. Proc. Natl. Acad. Sci. USA *94*, 2638–2641.

Baker, J., Liu, J.P., Robertson, E.J., and Efstratiadis, A. (1993). Role of insulin-like growth factors in embryonic and postnatal growth. Cell *75*, 73–82.

Bartlett, W.P., Li, X.S., Williams, M., and Benkovic, S. (1991). Localization of insulin-like growth factor-1 mRNA in murine central nervous system during postnatal development. Dev. Biol. *147*, 239–250.

Beck, K.D., Powell-Braxton, L., Widmer, H.R., Valverde, J., and Hefti, F. (1995). Igf1 gene disruption results in reduced brain size, CNS hypomyelination, and loss of hippocampal granule and striatal parvalbumin-containing neurons. Neuron *14*, 717–730.

Bhalla, A., Chicka, M.C., and Chapman, E.R. (2008). Analysis of the synaptotagmin family during reconstituted membrane fusion. Uncovering a class of inhibitory isoforms. J. Biol. Chem. *283*, 21799–21807.

Chen, W.R., and Shepherd, G.M. (1997). Membrane and synaptic properties of mitral cells in slices of rat olfactory bulb. Brain Res. *745*, 189–196.

Cheng, C.M., Mervis, R.F., Niu, S.L., Salem, N., Jr., Witters, L.A., Tseng, V., Reinhardt, R., and Bondy, C.A. (2003). Insulin-like growth factor 1 is essential for normal dendritic growth. J. Neurosci. Res. *73*, 1–9.

Fernandez-Chacon, R., Konigstorfer, A., Gerber, S.H., Garcia, J., Matos, M.F., Stevens, C.F., Brose, N., Rizo, J., Rosenmund, C., and Südhof, T.C. (2001). Synaptotagmin I functions as a calcium regulator of release probability. Nature *410*, 41–49.

Flannery, A.R., Czibener, C., and Andrews, N.W. (2010). Palmitoylation-dependent association with CD63 targets the Ca^{2+} sensor synaptotagmin VII to lysosomes. J. Cell Biol. *191*, 599–613.

Fukuda, M., Kanno, E., and Mikoshiba, K. (1999). Conserved N-terminal cysteine motif is essential for homo- and heterodimer formation of synaptotagmins III, V, VI, and X. J. Biol. Chem. *274*, 31421–31427.

Fukuda, M., Kowalchyk, J.A., Zhang, X., Martin, T.F., and Mikoshiba, K. (2002). Synaptotagmin IX regulates Ca^{2+}-dependent secretion in PC12 cells. J. Biol. Chem. *277*, 4601–4604.

Geppert, M., Goda, Y., Hammer, R.E., Li, C., Rosahl, T.W., Stevens, C.F., and Südhof, T.C. (1994). Synaptotagmin I: a major Ca2+ sensor for transmitter release at a central synapse. Cell *79*, 717–727.

Giacobini, M.M., Zetterstrom, R.H., Young, D., Hoffer, B., Sara, V., and Olson, L. (1995). IGF-1 influences olfactory bulb maturation. Evidence from anti-IGF-1 antibody treatment of developing grafts in oculo. Brain Res. Dev. Brain Res. *84*, 67–76.

Gustavsson, N., Lao, Y., Maximov, A., Chuang, J.C., Kostromina, E., Repa, J.J., Li, C., Radda, G.K., Sudhof, T.C., and Han, W. (2008). Impaired insulin secretion and glucose intolerance in synaptotagmin-7 null mutant mice. Proc. Natl. Acad. Sci. USA *105*, 3992–3997.

Gustavsson, N., and Han, W. (2009). Calcium-sensing beyond neurotransmitters: functions of synaptotagmins in neuroendocrine and endocrine secretion. Biosci. Rep. *29*, 245–259.

Gustavsson, N., Wei, S.H., Hoang, D.N., Lao, Y., Zhang, Q., Radda, G.K., Rorsman, P., Südhof, T.C., and Han, W. (2009). Synaptotagmin-7 is a principal Ca^{2+} sensor for Ca^{2+}-induced glucagon exocytosis in pancreas. J. Physiol. *587*, 1169–1178.

Ho, A., Morishita, W., Atasoy, D., Liu, X., Tabuchi, K., Hammer, R.E., Malenka, R.C., and Südhof, T.C. (2006). Genetic analysis of Mint/X11 proteins: essential presynaptic functions of a neuronal adaptor protein family. J. Neurosci. *26*, 13089–13101.

Hui, E., Bai, J., Wang, P., Sugimori, M., Llinas, R.R., and Chapman, E.R. (2005). Three distinct kinetic groupings of the synaptotagmin family: candidate sensors for rapid and delayed exocytosis. Proc. Natl. Acad. Sci. USA *102*, 5210–5214.

Isaacson, J.S., and Strowbridge, B.W. (1998). Olfactory reciprocal synapses: dendritic signaling in the CNS. Neuron *20*, 749–761.

Li, C., Davletov, B.A., and Südhof, T.C. (1995a). Distinct Ca^{2+} and Sr^{2+} binding properties of synaptotagmins. Definition of candidate Ca^{2+} sensors for the fast and slow components of neurotransmitter release. J. Biol. Chem. *270*, 24898–24902.

Li, C., Ullrich, B., Zhang, J.Z., Anderson, R.G., Brose, N., and Südhof, T.C. (1995b). Ca^{2+}-dependent and -independent activities of neural and non-neural synaptotagmins. Nature *375*, 594–599.

Li, J., Xiao, Y., Zhou, W., Wu, Z., Zhang, R., and Xu, T. (2009). Silence of Synaptotagmin VII inhibits release of dense core vesicles in PC12 cells. Sci. China C Life Sci. *52*, 1156–1163.

Liu, J.P., Baker, J., Perkins, A.S., Robertson, E.J., and Efstratiadis, A. (1993). Mice carrying null mutations of the genes encoding insulin-like growth factor I (Igf-1) and type 1 IGF receptor (Igf1r). Cell *75*, 59–72.

Lynch, K.L., and Martin, T.F. (2007). Synaptotagmins I and IX function redundantly in regulated exocytosis but not endocytosis in PC12 cells. J. Cell Sci. *120*, 617–627.

Martinez, I., Chakrabarti, S., Hellevik, T., Morehead, J., Fowler, K., and Andrews, N.W. (2000). Synaptotagmin VII regulates Ca^{2+}-dependent exocytosis of lysosomes in fibroblasts. J. Cell Biol. *148*, 1141–1149.

Maximov, A., Pang, Z.P., Tervo, D.G., and Südhof, T.C. (2007). Monitoring synaptic transmission in primary neuronal cultures using local extracellular stimulation. J. Neurosci. Methods *161*, 75–87.

Maximov, A., and Südhof, T.C. (2005). Autonomous function of synaptotagmin 1 in triggering synchronous release independent of asynchronous release. Neuron *48*, 547–554.

Miesenböck, G., De Angelis, D.A., and Rothman, J.E. (1998). Visualizing secretion and synaptic transmission with pH-sensitive green fluorescent proteins. Nature *394*, 192–195.

Mittelstaedt, T., Seifert, G., Alvarez-Baron, E., Steinhauser, C., Becker, A.J., and Schoch, S. (2009). Differential mRNA expression patterns of the synaptotagmin gene family in the rodent brain. J. Comp. Neurol. *512*, 514–528.

Pang, Z.P., Cao, P., Xu, W., and Südhof, T.C. (2010). Calmodulin controls synaptic strength via presynaptic activation of calmodulin kinase II. J. Neurosci. *30*, 4132–4142.

Pang, Z.P., Shin, O.H., Meyer, A.C., Rosenmund, C., and Südhof, T.C. (2006). A gain-of-function mutation in synaptotagmin-1 reveals a critical role of Ca^{2+}-dependent soluble N-ethylmaleimide-sensitive factor attachment protein receptor complex binding in synaptic exocytosis. J. Neurosci. *26*, 12556–12565.

Rosenmund, C., and Stevens, C.F. (1996). Definition of the readily releasable pool of vesicles at hippocampal synapses. Neuron *16*, 1197–1207.

Rotwein, P., Burgess, S.K., Milbrandt, J.D., and Krause, J.E. (1988). Differential expression of insulin-like growth factor genes in rat central nervous system. Proc. Natl. Acad. Sci. USA *85*, 265–269.

Schonn, J.S., Maximov, A., Lao, Y., Südhof, T.C., and Sorensen, J.B. (2008). Synaptotagmin-1 and −7 are functionally overlapping Ca^{2+} sensors for exocytosis in adrenal chromaffin cells. Proc. Natl. Acad. Sci. USA *105*, 3998–4003.

Schoppa, N.E., Kinzie, J.M., Sahara, Y., Segerson, T.P., and Westbrook, G.L. (1998). Dendrodendritic inhibition in the olfactory bulb is driven by NMDA receptors. J. Neurosci. *18*, 6790–6802.

Scolnick, J.A., Cui, K., Duggan, C.D., Xuan, S., Yuan, X.B., Efstratiadis, A., and Ngai, J. (2008). Role of IGF signaling in olfactory sensory map formation and axon guidance. Neuron *57*, 847–857.

Shin, O.H., Xu, J., Rizo, J., and Südhof, T.C. (2009). Differential but convergent functions of Ca^{2+} binding to synaptotagmin-1 C2 domains mediate neurotransmitter release. Proc. Natl. Acad. Sci. USA *106*, 16469–16474.

Sorensen, J.B., Fernandez-Chacon, R., Südhof, T.C., and Neher, E. (2003). Examining synaptotagmin 1 function in dense core vesicle exocytosis under direct control of Ca^{2+}. J. Gen. Physiol. *122*, 265–276.

Südhof, T.C., Czernik, A.J., Kao, H.T., Takei, K., Johnston, P.A., Horiuchi, A., Kanazir, S.D., Wagner, M.A., Perin, M.S., De Camilli, P., et al. (1989). Synapsins: mosaics of shared and individual domains in a family of synaptic vesicle phosphoproteins. Science *245*, 1474–1480.

Südhof, T.C., and Rothman, J.E. (2009). Membrane fusion: grappling with SNARE and SM proteins. Science *323*, 474–477.

Sugita, S., Shin, O.H., Han, W., Lao, Y., and Südhof, T.C. (2002). Synaptotagmins form a hierarchy of exocytotic Ca^{2+} sensors with distinct Ca^{2+} affinities. EMBO J. *21*, 270–280.

Trombley, P.Q., and Westbrook, G.L. (1990). Excitatory synaptic transmission in cultures of rat olfactory bulb. J. Neurophysiol. *64*, 598–606.

Vicario-Abejon, C., Yusta-Boyo, M.J., Fernandez-Moreno, C., and de Pablo, F. (2003). Locally born olfactory bulb stem cells proliferate in response to insulin-related factors and require endogenous insulin-like growth factor-I for differentiation into neurons and glia. J. Neurosci. *23*, 895–906.

Vrljic, M., Strop, P., Ernst, J.A., Sutton, R.B., Chu, S., and Brunger, A.T. (2010). Molecular mechanism of the synaptotagmin-SNARE interaction in Ca^{2+}-triggered vesicle fusion. Nat. Struct. Mol. Biol. *17*, 325–331.

Wang, P., Chicka, M.C., Bhalla, A., Richards, D.A., and Chapman, E.R. (2005). Synaptotagmin VII is targeted to secretory organelles in PC12 cells, where it functions as a high-affinity calcium sensor. Mol. Cell. Biol. *25*, 8693–8702.

Xu, J., Mashimo, T., and Südhof, T.C. (2007). Synaptotagmin-1, −2, and −9: Ca^{2+} sensors for fast release that specify distinct presynaptic properties in subsets of neurons. Neuron *54*, 567–581.